DESTRUCTIVE STRONG GROUND MOTION IN MEXICO CITY: SOURCE, PATH, AND SITE EFFECTS DURING GREAT 1985 MICHOACÁN EARTHQUAKE

BY M. CAMPILLO, J. C. GARIEL, K. AKI, AND F. J. SÁNCHEZ-SESMA

ABSTRACT

Simultaneous consideration of source, path, and site effects on ground motion during the Michoacán earthquake of 1985 allows us to draw coherent conclusions regarding the roles played for the disaster in Mexico City by the rupture process, the mode of propagation of the waves between the epicentral zone and Mexico City, and the local amplification. In contrast to the horizontal component which showed dramatic amplification for the 2 to 3 sec motion at lake sediment sites, we observe almost identical vertical displacement seismograms containing ripples with 2 to 3 sec period throughout the Mexico City valley whether the recording site is on the lake sediments or on hard rock. We, therefore, conclude that the 2 to 3 sec motion responsible for the destruction of Mexico City was present in the incident field. After performing a phase analysis, we interpret the signal as the superposition of long-period Rayleigh waves and short-period Lg with a dominant period of about 3 sec. The analysis of the teleseismic records indicates that the radiation of this event is enhanced for waves around the 3 sec period. Except in the case of stations for which an anomalous path effect is suspected, the records present ripples appearing a few seconds after the beginning of the signal. The characteristics of near-fault records show that the rupture process consists of the growth of a smooth crack. The numerical simulation indicates that the 3 sec period ripples can be explained by a series of changes of the rupture front velocity. We examine two alternative source models associated with different crustal models to explain the characteristics of the vertical displacements recorded in Mexico City. Our preferred model attributes the cause of the enhanced 3 sec motion to the irregularity in the rupture propagation in addition to the effect of the local conditions in Mexico City. This interpretation leads to a very coherent scenario of what happened from the start of the failure on the fault up to the destruction in Mexico City. This example illustrates the need to consider simultaneously source, path, and site effects in order to understand strong ground motions.

INTRODUCTION

Why did the 19 September 1985 Michoacán earthquake with $M_s = 8.1$ show low peak ground acceleration in the epicentral area (Anderson *et al.*, 1986) and yet caused severe damage in Mexico City?

The aim of this report is to show that a complete answer requires simultaneous consideration of source and path effect in addition to the local site effect. We will present conclusions coming from different types of seismic data and develop a complete, coherent scenario of what happened on 19 September 1985 when the so-called Michoacán gap broke, emitting seismic waves that finally severely damaged Mexico City and left more than 100,000 people homeless.

We will discuss the role played by each of the source, path, and site effects using strong ground motions recorded in Mexico City, teleseismic data, and strong ground motions recorded very close to the fault. First, we shall identify the type of seismic waves incident upon the Mexico City valley.

1718

VERTICAL DISPLACEMENTS IN MEXICO CITY

One of the causes of the severe damage in Mexico City is the site effect due to the presence of extremely soft shallow lake sediments. This phenomenon has been studied in detail by various authors (e.g., Romo and Seed, 1986; Bard *et al.*, 1988) who attributed the cause of the damage to a double resonance of building and lake sediments at around the 3 sec period. The amplitude and duration of the ground motion can be amplified also by the presence of a deep basin whose resonance period is also around 3 sec (Bard *et al.*, 1988), and by the effect of small scale irregularities of the superficial soft layer (Campillo *et al.*, 1989). The complete description of the causes of this disaster, however, requires simultaneous consideration of source and path effects in addition to the local site effect. Taking into account the characteristics of the teleseismic records, Singh *et al.* (1989) concluded that the earthquake source made an anomalous additional contribution to the ground motion around the period of 3 sec. The ripples of period between 2 and 4 sec discussed by Singh and his colleagues can be seen on the displacement records obtained in the region of Mexico City. While the horizontal components of the displacement are strongly dependent on the characteristics of the soil beneath the stations, the vertical displacement records show nearly identical waveforms and amplitudes at all stations with variable local site conditions (Fig. 1). Stations TACY and CUIP are located on the hill region where the soil consists of compact pre-Chichinautzin sedimentary layer and basaltic lava flows, respectively. Stations SCT and CDAF are in the lake region covered by the soft lacustrine clay deposit. Station SXVI is located in the transition zone between the above two regions. Clearly the 3 sec ripples, superposed with a long-period pulse and observed at all these sites are not due to local site conditions but represent the characteristics of waves incident from the depth.

In order to determine precisely the nature of the wave field incident on the basin of Mexico City we performed a multi-channel phase analysis of these displacement records. The detail of this analysis is given by Campillo *et al.* (1988), and their main results are summarized here. First, the eigenvalue decomposition indicated that each of the prominent period bands (i. e., around 12 sec and 3 sec) is associated with a single mode of propagation. Since the absolute time is not known precisely, we have deduced a time delay from the relative phase measured between these two narrow period bands. The time delay of the long-period pulse relative to the ripples increases with the distance from the earthquake source (Fig. 2). Since the long-period waves are likely propagating from the source, the above results support that the ripples are also coming from the source.

The interpretation of the nature of these arrivals is difficult and non-unique. A straightforward interpretation, based on the usual characteristics of short period records along continental paths, consists of identifying the long-period pulse with the Rayleigh wave and the ripples with the *Lg* wave train. Various arguments can be invoked to support this hypothesis. First is the fact that for other records in Mexico City of earthquakes along the subduction, *Lg* is the prominent phase. Second is that both energetic frequency bands are associated with distinctly different modes of propagation. This point refutes the hypothesis of body waves having a bimodal spectrum. It is well known that Rayleigh waves are dominant at long periods while the *Lg* spectrum strongly decreases for periods greater than a few seconds (Herrmann and Kijko, 1983). An analysis of the particle motion performed by Quaas *et al.* (personal comm.) shows that the long-period pulse has a polarization
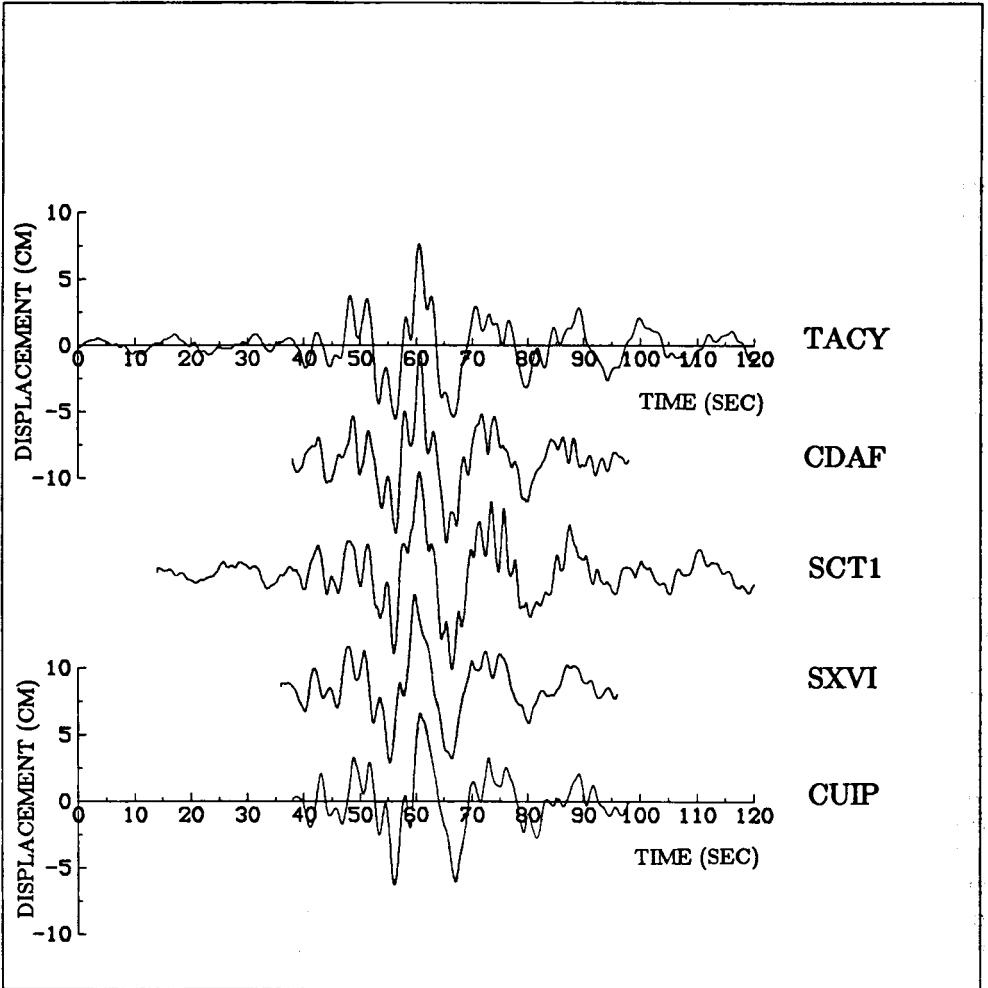
FIG. 1. Examples of vertical displacement records obtained at different sites in Mexico City (after Mena *et al.*, 1986).

which corresponds to a Rayleigh wave. Finally, this hypothesis is also supported by the fact that the larger phase velocity is associated with the higher frequency (Campillo *et al.*, 1988).

As shown later, the identification of the incident waves as *Lg* that will be strongly amplified by the site effects explains satisfactorily the duration of the seismograms recorded in Mexico City. The effect of source complexity on duration is weak as compared to the effect of reverberation within the crust during the propagation. The attenuation of *Lg* with distance is also weaker than that of body waves because *Lg* consists of guided waves. Thus, the path effect contributes to low attenuation and long duration of ground motions with period around 3 sec which caused the disaster in Mexico City.

The coupling between the source and path effects governing the strong motion is particularly strong in the case of the Michoacán earthquake, and a correct determination of the source process depends on our knowledge about the structure of the crust along the path to Mexico City. The crustal structure has been studied by
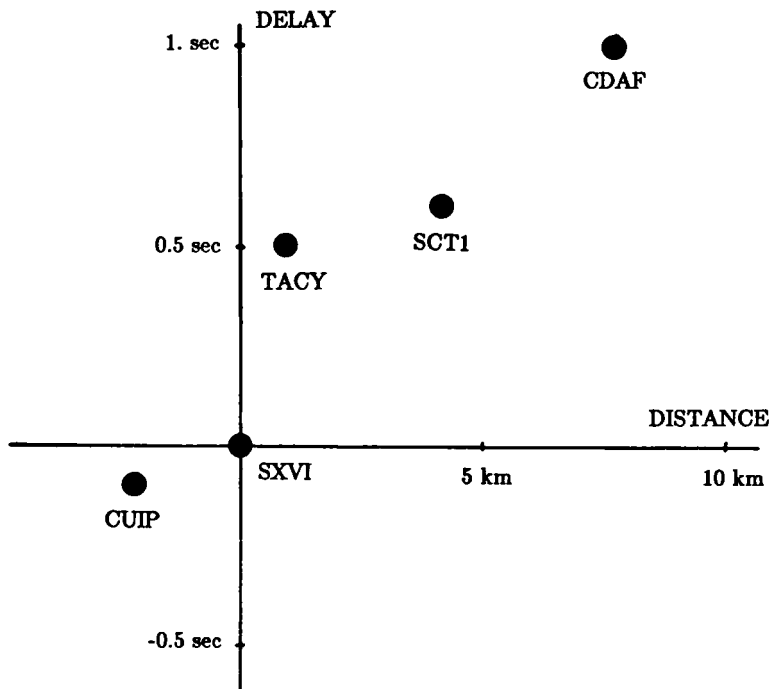
FIG. 2. Time delays deduced from the phase measurements as a function of the apparent distance from the fault zone.

Steinhart and Meyer (1961) in Central Mexico and by Valdes *et al.* (1986) in Oaxaca. Both results are in agreement on the depth of the Moho at about 45 km. Valdes *et al.* (1986) deduced from their refraction profile the existence of a thick surface layer of relatively low velocity materials (V_P = 4.5 km/sec) beneath Oaxaca. We found that the question of whether this structure exists along the path between the source zone of the Michoacán earthquake and Mexico City is of crucial importance for the definite conclusion on the whole process.

A First Interpretation

Considering a flat crustal structure directly deduced from the results obtained in Oaxaca by Valdes *et al.* (1986) (Table 1), we have modeled the vertical displacement records observed in Mexico City. The local geology was neglected since we have shown that its effect is very weak for the vertical displacements. The general feature of the source process of the Michoacán earthquake was inferred from teleseismic P waveforms (e. g., Eissler *et al.*, 1986; UNAM Seismology Group, 1986; Mendoza and Hartzell, 1988). The source consists of at least two subevents separated in space by about 80 km. The second subevent occured 26 sec after the first. The existence of a third subevent has been proposed by Houston and Kanamori (1986) and Mendoza and Hartzell (1988). In our schematic modeling, we represent the earthquake by three point sources whose location, timing, and seismic moments are those obtained by Houston and Kanamori (1986). The source durations of the three events are assumed to be 16 sec, 16 sec, and 3 sec. This last value is much shorter than proposed by Houston and Kanamori (a rise time of 10 sec for the third event) and plays a prominent part in this interpretation. The focal mechanism considered is the same for the three subevents. Following the results of Houston and Kanamori

(1886) and Riedesel *et al.* (1986), we chose the values of dip and rake to be respectively 15° and 76°. Figure 3 shows the synthetics, convolved with the high-pass Ormsby filter, used for the processing of the data. The good agreement obtained between the amplitudes of synthetic and actual vertical displacement confirms the moment values of Houston and Kanamori and therefore the "long period description" of the earthquake. The long-period pulse is composed of Rayleigh waves from the first two subevents. We found that the entire energy at period 3 sec is coming

TABLE 1
CRUSTAL MODEL USED TO COMPUTE THE SYNTHETICS SHOWN IN FIGURE 3

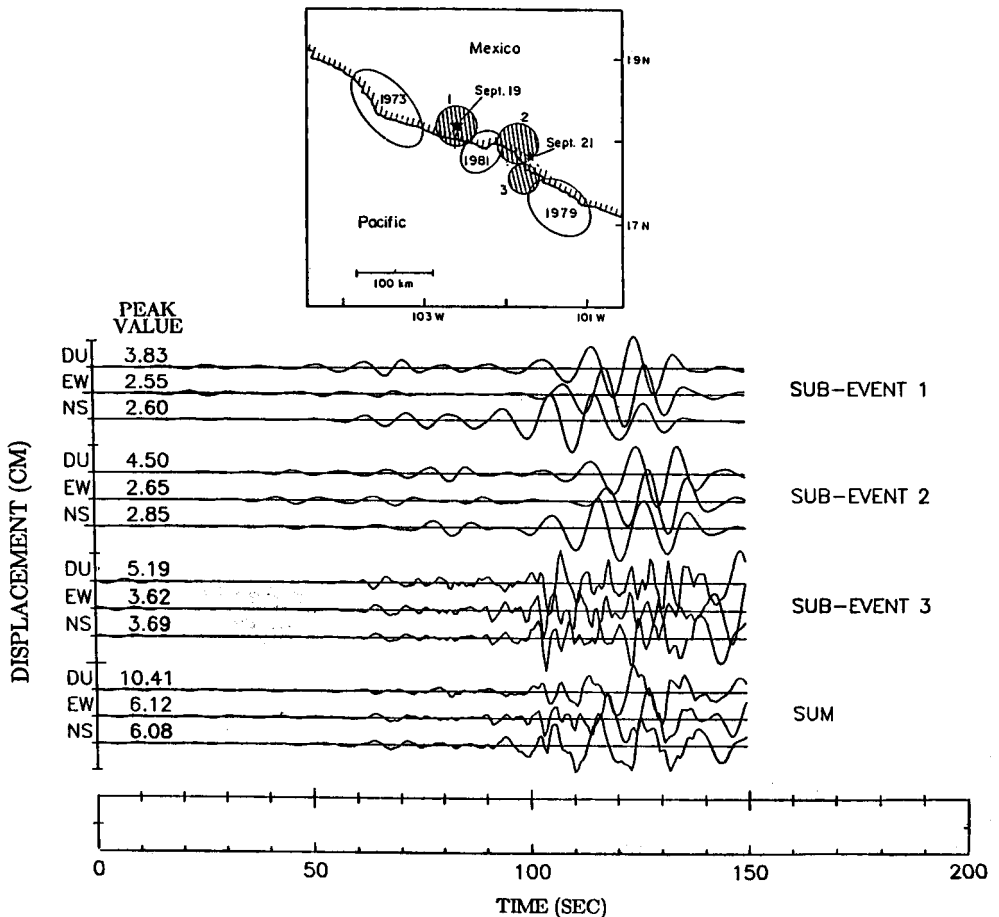| Layer	Thickness (km)	V_P(km/sec)	V_s(km/sec)	Density (gm/cm³)	Q_P	Q_s
1	5.	4.3	2.53	2.67	800	500
2	10.	5.7	3.3	2.77	800	500
3	15.	6.8	4.03	3.09	800	500
4	15.	7.	4.1	3.09	800	500
5	0.	8.2	4.82	3.3	800	500

FIG. 3. Geometry of the three subevents (crosshatched) proposed by Houston and Kanamori (1986) and synthetic seismograms corresponding to records in Mexico City. The synthetics shown are obtained in the crustal model given in Table 1 for each subevent; their sum is also plotted. The synthetics are convolved by a Ormsby filter as described by Mena *et al.* (1986). See text for details of the model.

as *Lg* from the third subevent. Because of the relative group velocity of *Lg* and Rayleigh wave in this model, we cannot allow that the ripples are coming from the first subevent and at the same time produce a waveform similar to those observed in Mexico City, where the long-period pulse arrives only 15 sec after the 3 sec ripples. On the other hand, we have no other evidence supporting a strong high-frequency emission from the southern part of the fault (the third event), although Mendoza and Hartzell (1988) found a possible strike-slip event located in this region without constraints on its dynamic characteristics, and a strike slip mechanism for the third subevent will not change significantly the numerical result shown on Figure 3. Furthermore, neither the intensity map nor the observed peak values of acceleration along the coast indicate a specific source of high frequency waves in the south of the rupture zone (Martínez and Javier, 1985).

This interpretation relies on a crustal model that is not directly applicable to the path between the Michoacán epicenter to Mexico City. The validity of this interpretation has to be tested by additional information.

TELESEISMIC *P* WAVEFORMS

The most important characteristics of the teleseismic waveform relevant to the damage in Mexico City, namely, ripples with periods from 2 to 4 sec, are found on the intermediate-period range records and broadband records from digital stations of the DWWSSN, SRO, RSTN, GEOSCOPE, and NARS networks. Observed vertical intermediate-period records have been summarized in a USGS Open-file report (Zirbes *et al.*, 1985). The superposition of a long-period pulse and an oscillation with a few seconds period is clearly seen in *P* waves recorded at many stations, as shown by Houston and Kanamori (1986) and Singh *et al.* (1989).

The ripples are, however, missing for the stations RSTN, GDH, RSON, RSNY, and RSSD. These stations are located in the azimuth range between north and northeast from the epicenter with the take-off angles of the direct *P* wave between 24° and 30° (Fig. 4). This suggests a possible path effect for the missing ripples. Actually, the paths corresponding to these records go through the dipping slab and through a zone where the deep roots of transmexican volcanic range are probably located. These structures may be responsible for strong scattering and attenuation. In addition to the above presumed path effect due to near-source anomalous structure, there may be near-receiver path effects on the teleseismic waveform. An example is shown in Figure 5 where we compared broadband records from the Michoacán earthquake obtained in Grafenberg, Germany, and Saint-Sauveur, France. These two stations are relatively close both in distance and azimuth (2° and 6° apart, respectively) but the relative amplitudes of the ripples to the long-period signal are very different. This can be due to the heterogeneous crust under the stations. With regard to the ripples, it is important to note that, even at these relatively low frequencies, we cannot neglect near-source or near-station path effects to draw firm conclusions about the source process by comparing teleseismic *P*-wave records from different stations or from different earthquakes.

We may, however, conclude in this case that except for the particular stations where anomalies of propagation are suspected the ripples are present and their position with respect to the long-period pulse does not show any systematic azimuthal variations. Their arrival is almost simultaneous with the long-period *P* wave. Analyzing most of the avaliable data, Singh *et al.* (1989) have computed spectral ratios between records of the 1985, Michoacán earthquake and records of
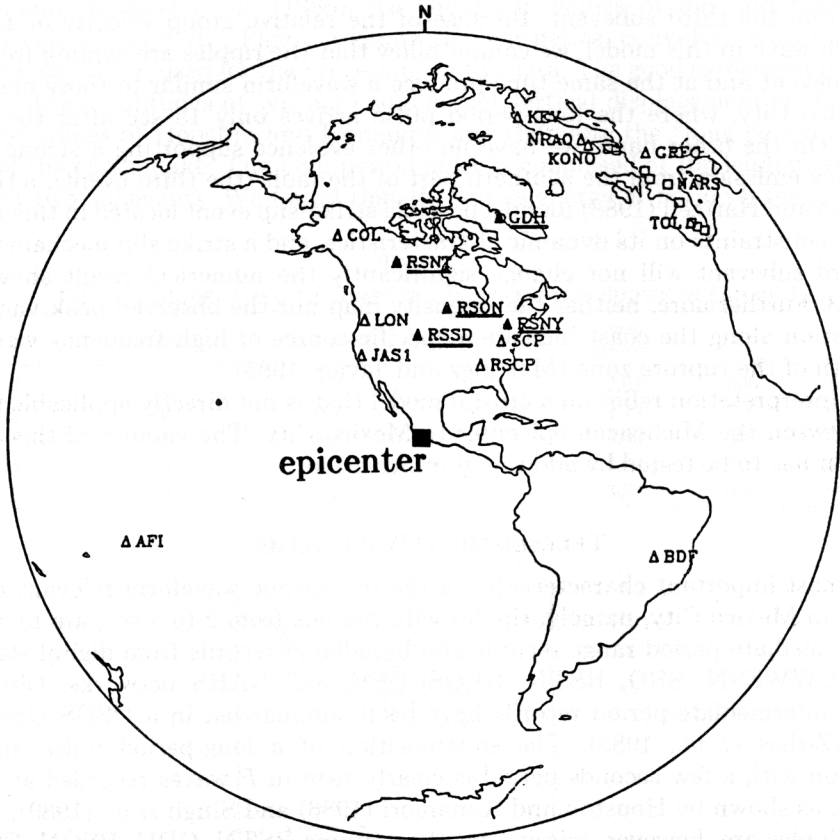
FIG. 4. Stations whose records are presented in Zirbes *et al.* (1985) for the 19 September 1985 Michoacán, Mexico, earthquake. The stations where the ripples are missing are indicated by a black triangle; the station name abbreviations are also underlined.

several other events which occurred along the Mexican subduction zone. They concluded that, overall, the Michoacán earthquake exhibits an anomalously large teleseismic radiation in the northeast quadrant for frequencies between 0.3 and 0.7 Hz, relative to other events and larger than that predicted by the ω^{-2} source model in that frequency range.

Our conclusion coming from the teleseismic data is that the radiation from this earthquake is characterized by enhanced waves of the 3 sec period which have originated shortly after the beginning of the rupture process. This conclusion clearly contradicts our first interpretation described in the preceding section.

RUPTURE PROCESS FROM NEAR SOURCE GROUND MOTION.

The ground motion during the earthquake has been recorded at stations directly above the fault plane (Anderson *et al.*, 1986). Station Caleta de Campos is located close to the epicenter and therefore shows clearly the effect of the rupture front passing beneath the receiver. In this case, the vertical displacement record represents approximately the displacement in a direction perpendicular to the rupture surface (i. e., tranverse motion). The observed waveform is characterized by a smooth simple ramp with a very slight overshoot as shown in Figure 6. This record
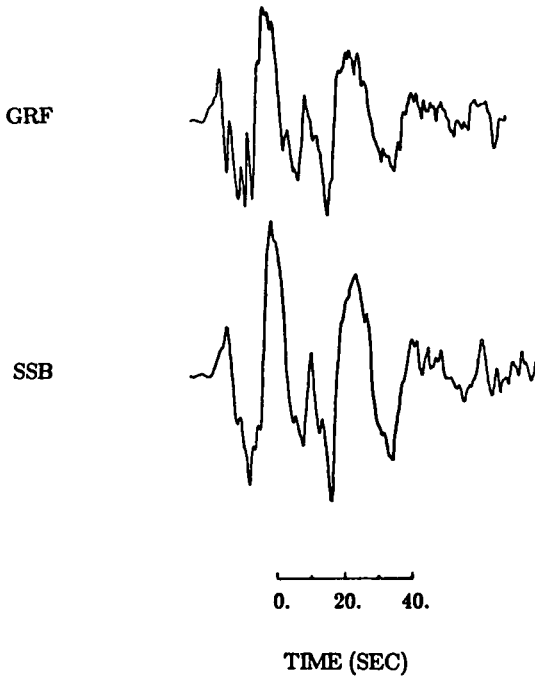
GRF

SSB

```
 0.    20.    40.
```

TIME (SEC)

FIG. 5. Comparison of broadband records obtained at two close stations. Grafenberg, Germany (after Singh *et al.*, 1989) and Geoscope station Saint Sauveur (France).

can be compared with the observation of the transverse displacement at station 2 during the 1866 Parkfield, California, earthquake which shows a strongly impulsive shape. Aki (1968) has shown that a simple propagating dislocation model can explain satisfactorily the waveform observed in Parkfield. This waveform is very much dependent on the type of displacement discontinuity occurring on the fault plane (Aki and Richards, 1980): a constant stress-drop crack model and a uniform dislocation model can be distinguished from the shape of the tranverse displacement. In order to test the sensitivity of the near-field waveforms on the slip function in the particular case of the Michoacán earthquake, we computed synthetic seismograms for different source models. We follow the conclusions of Houston and Kanamori (1986) in considering the existence of a first subevent which extends beneath Caleta de Campos. The slip occurred on a fault patch bounded by the previously broken zones of the 1981 Playa Azul earthquake in the south and 1973 Colima earthquake in the north. We assume that the rupture initiated at 17 km depth, 20 km northeast from the station as indicated by hypocentral locations. Because the second rupture patch is located at least 60 km away from the station, we will consider only the effect of the first subevent in our computation. We consider two models of rupture for our simulations. The first consists of a dislocation model on a square fault plane (Fig. 7a). The rupture initiates at the center of the northern edge of the fault and then spreads isotropically up dip until it reaches the limits of the fault. The displacement discontinuity is of the same form at all locations $\vec{x}$ on the broken area and is given by:

$$\Delta u(\vec{x}, t) = u_0 \frac{1. + \tanh((t - t_r)/t_0)}{2}$$
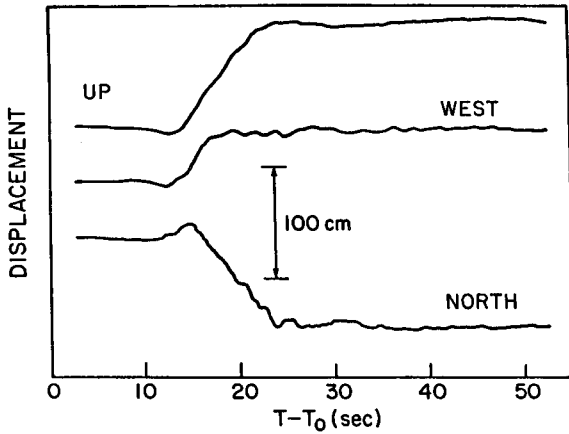
FIG. 6. Displacement records obtained at Caleta de Campos, just above the fault zone (after Anderson *et al.*, 1986).

with $t_r = |(\vec{x} - \vec{x}_h)| / V_R$ and where V_R and $\vec{x}_h$ denote the rupture velocity and the location of the hypocenter. u_0 is the final slip. The rise time t_0 is chosen as 4 sec. This model represents a propagating uniform dislocation and is essentially the same as those used by Aki (1968) to explain the transverse displacement observed at station 2 during the Parkfield earthquake or by Bouchon (1981) to model the ground motion during the 1978 Coyote Lake, California, earthquake.

The second model we investigated is a crack model with unilateral propagation. The numerical study of isotropic crack propagation performed by Madariaga (1976) shows that the self similar crack model of Kostrov (1964) gives a very good approximation of the source function until the rupture stops, when the healing phase appears. In order to study the effect of the passage of the rupture front, we therefore built a model based directly on the self similar solution. The rupture front is depicted at different times in Figure 7b while Figure 7c shows the displacement discontinuity, which corresponds at each time to the elliptical static solution. The displacement discontinuity on the fault is given by:

$$\Delta u(\vec{x}, t) = 0 \qquad\qquad\qquad t < t_0(\vec{x})$$

$$\Delta u(\vec{x}, t) = u_0\sqrt{V_R^2 t^2 - \vec{x}^2} \quad t_0(\vec{x}) < t < t_1$$

$$\Delta u(\vec{x}, t) = u_0\sqrt{V_R^2 t_1^2 - \vec{x}^2} \qquad t > t_1$$

with

$$t_0(\vec{x}) = \frac{|\vec{x}|}{V_R} \quad \text{and} \quad t_1 = \frac{r}{V_R}$$

The symbol r is the final radius reached by the crack and $\vec{x}$ is the location of the point considered on the fault plane with respect to the center of the circle representing the rupture front.

The computations were carried out using the discrete wavenumber representation of seismic wavefields (Bouchon and Aki, 1977; Bouchon, 1978). The fault is represented by an array of equidistant point sources. The interval between elementary
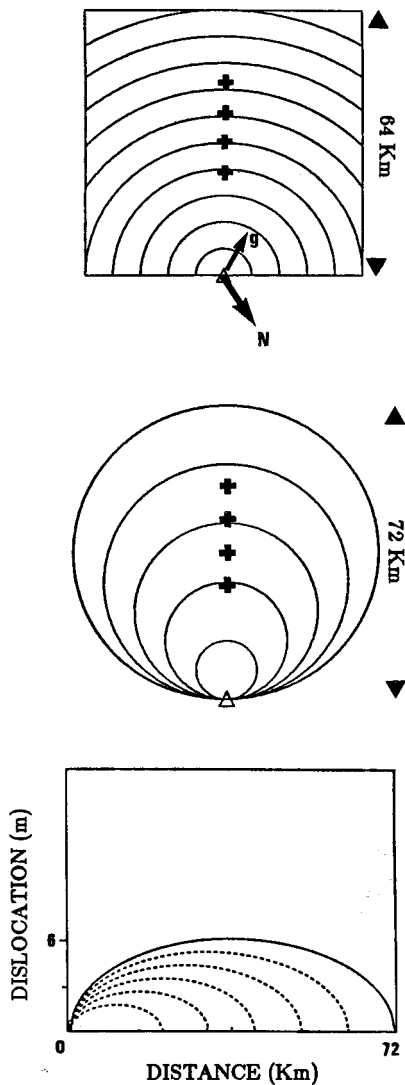
FIG. 7. (a) Geometry considered for the model of dislocation. Arrows N and g denote respectively the direction of the North and of the slip on the fault. The lines indicate the position of the rupture front at equal time intervals. The crosses are the locations of the receivers. (b) Same as (a) for the crack model. The surface of the fault is the same as for the dislocation. (c) Growth of an asymmetric crack. The lines indicate the slip along the fault at equal intervals time.

sources is chosen to be one sixth of the shortest wavelength considered in the computations. This method presents the advantage of allowing an exact analytical description of any slip function. The location of the points above the fault where the displacements are computed are presented on Figure 7.

We have assumed a constant direction of slip on the entire fault. Following the results of Eissler *et al.* (1986) and Riedesel *et al.* (1986), we chose the values of dip and rake to be respectively 15° and 76°. In the absence of information about the structure of the crust, we have performed our computation for an elastic half-space whose characteristics are the following: a *P*-wave velocity of 5.7 km/sec, a *S*-wave velocity of 3.35 km/sec, and a density of 2.77. The rupture velocity is equal to 0.75 V_S. The seismic moment of this first subevent represents about 45% of the total

moment (Houston and Kanamori, 1986), that is, according to the evaluation of the seismic moment of Ekstrom and Dziewonski (1986), about $0.5\ 10^{28}$ dyne-cm Considering a surface area of the rupture zone equal to 4096 km², the final value of the average slip to be used in the computations should be 4 m.

Without actual constraints on the limits of the rupture, and on the position of the station with respect to them, we have computed the displacements at four receivers on the axis of symmetry of the fault model. We therefore shall limit our discussion on the effect of the rupture front passing beneath the station. The synthetic displacements are displayed on Figure 8a and b for the models of dislocation and crack. Whichever receiver is considered, the displacements corresponding to each model show very specific characteristics, confirming that the passing of the rupture front is the prominent event. As suspected, the displacement produced in the dislocation model exhibits a clear overshoot before stabilizing to the static value. On the contrary, the vertical displacements obtained with the crack model are characterized by a smooth ramp, very similar to the shape observed on actual records. The static value of displacement obtained in this model is dependent on circular crack in a half-space is an oversimplified model of the reality we did not try to fit the observed value of displacement precisely, but were satisfied by the good agreement obtained using an approximate geometry and realistic seismic moment and slip. In fact, the computed static displacements are very close to the observed values for a slip on the fault similar to the one inferred from teleseismic records by Mendoza and Hartzell (1988) for this part of the rupture zone. This
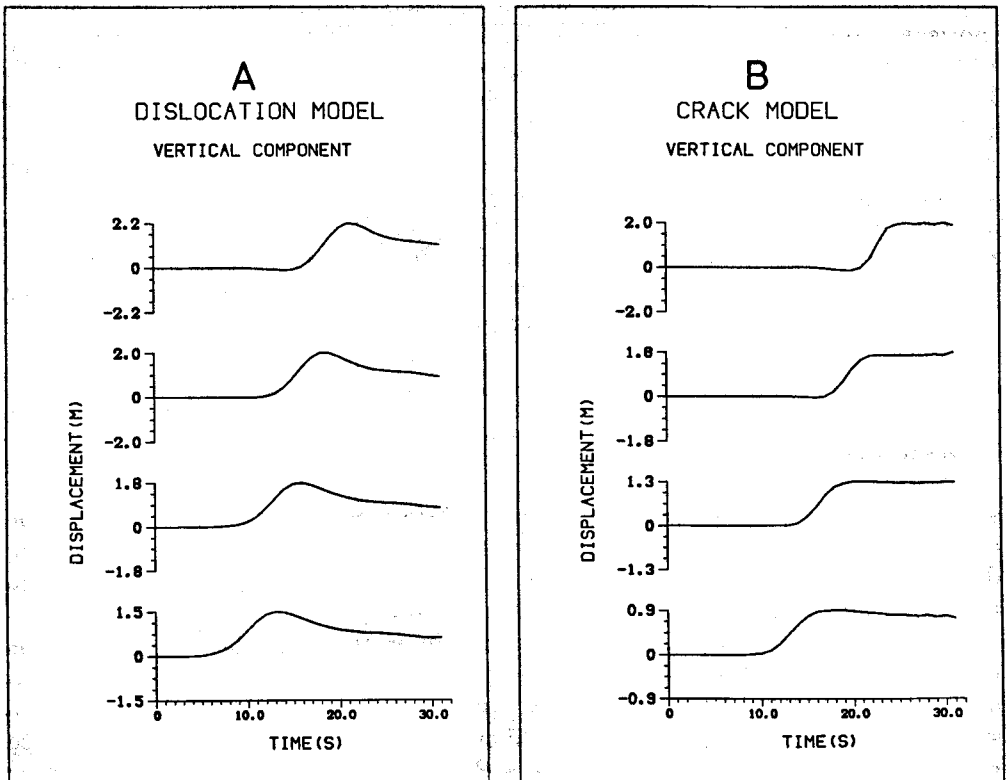

FIG. 8. Synthetic displacements obtained in the fault-receiver configuration described in Figure 3 for a dislocation model (a) and for a crack model (b).

result indicates that the first part of the rupture process during the Michoacán earthquake corresponds to the growth of a smooth crack. This result is in agreement with a similar study by Yomogida (1988) who used a finite-difference method. This crack model, however, cannot explain the teleseismic P waveforms characterized by ripples arriving shortly after the begining of the signal. The ground velocity records at Caleta de Campos (Fig. 9a) indicates that the ripples are present in the near-field motion. In order to explain this complexity and, at the same time, to account for the smooth waveform of the displacement, we propose a model of a self similar crack whose rupture velocity changes. In this model the complexity of the ground motion is due entirely to the kinematics of the rupture front while the distribution of final slip on the fault surface remains the same to that of a smooth crack. Simple examples of the results obtained with this model are presented in Figure 9b–d with the corresponding kinematics of the rupture front. We have verified that the vertical displacements show the same characteristics as for a smooth crack (i. e., absence of overshoot).

These results indicate that the ripples can be explained by a series of changes of the rupture velocity. An extreme case is a crack that completly stops, then restarts and repeats the process. Such a phenomenon has been analytically investigated by Ida (1973) and corresponds to the behavior of a fault on which dynamic failure and creep are occuring simultaneously. As shown numerically by Ida, even in an
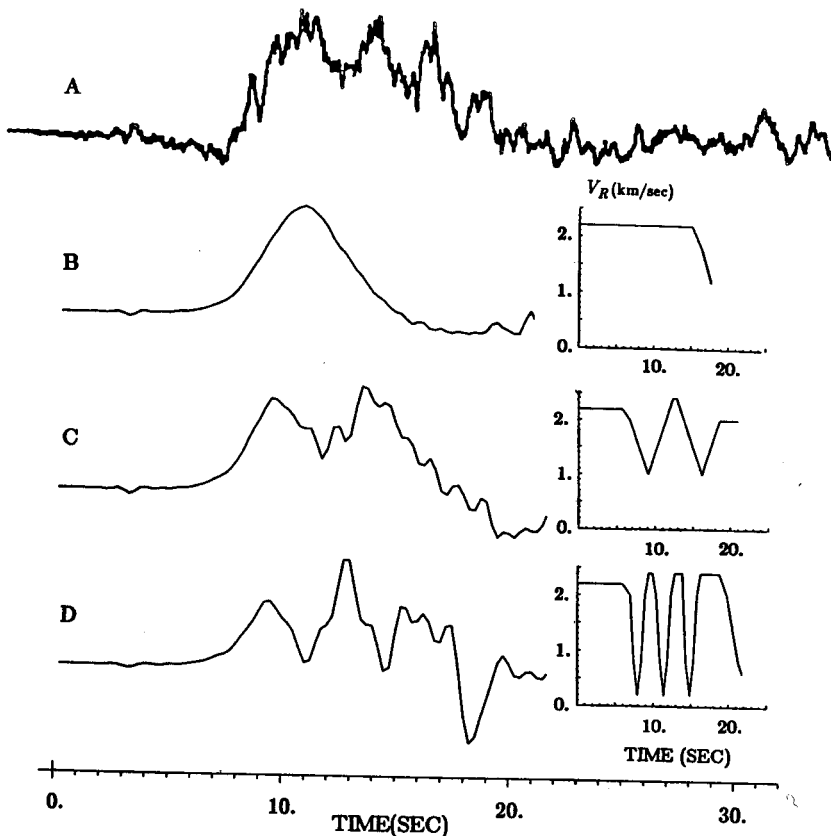

FIG. 9. (a) Vertical velocity records at Caleta de Campos. (b), (c), and (d) Synthetic seismograms obtained for the kinematics of the rupture front shown in the figure.

homogeneous medium this process of rupture front acceleration-deceleration is characterized by a unique time scale that suggests an apparent periodicity. This interpretation of the rupture process which generates the narrow-band ripples observed in Mexico City does not require postulation of an *ad hoc* periodic structure on the plate interfaces, such as a series of equidistant barriers and asperities. Since the ripples are observed in the teleseismic records as well as in the near-source observations, we must conclude after Kasahara (1955) and Singh *et al.* (1989) that they are due to a source effect. Our model is based essentially on the irregular growth of a simple crack and does not imply the existence of barriers (Das and Aki, 1977) which eventually break. The barrier failure would produce strong high frequency radiation that would be in contradiction with the low level of acceleration observed along the coast (Anderson *et al.*, 1986): a maximum of 0.2 g on the horizontal component. This is unusually low because according to Campbell (1981) or Kawashima *et al.* (1984), a value of peak acceleration of 0.8 g is expected for an event of this magnitude at 20 km from the fault.

A SECOND INTERPRETATION OF THE VERTICAL GROUND DISPLACEMENT IN MEXICO CITY

The conclusions that were drawn from the teleseismic records and the near-source observations lead us to discard our first assumption of the existence of a third subevent that was responsible for the 3 sec ripples observed in Mexico City. Because of the different group velocities of *Lg* and Rayleigh waves in the crustal model deduced from the results of Valdes *et al.* (1986) in Oaxaca (see Fig. 3), we cannot expect to model the simultaneous arrival of *Lg* and Rayleigh wave by assuming that the ripples are emitted at the beginning of the rupture process. Nevertheless, because of the presence of the volcanic complexes of Sierra Madre del Sur and transmexican volcanic range along the path, we may assume that the upper layer consists of thick andesitic materials. Consequently, the velocities in the upper layer can be expected to be higher than those proposed by Valdes *et al.* This point leads us to consider a crustal model as presented in Table 1 in which the surficial layer has been removed and the second layer continued up to the surface (Table 2). Under this assumption, we can test the hypothesis that the 3 sec ripples are emitted shortly after the beginning of the process. Thus, we will model the records in Mexico City considering a simple point source with a bimodal spectrum with dominant periods at 3 and 12 sec. Following Singh *et al.* (1989) we assume that the ripples start to be emitted 8 sec after the begining of the rupture. Because the rupture was propagating in a direction roughly opposite to Mexico City, the difference in location will result in a relative delay of about 6 sec with respect to the start of the long-period pulse. In the time domain, the 3 sec period excitation consists of two Ricker pulses separated by 7 sec, which corresponds to the apparent

TABLE 2

CRUSTAL MODEL USED TO COMPUTE THE SYNTHETICS SHOWN IN FIGURE 10

Layer	Thickness (km)	Vp(km/sec)	Vs(km/sec)	Density (gm/cm^3)	Qp	Qs
1	15.	5.7	3.3	2.77	800	500
2	15.	6.8	4.03	3.09	800	500
3	15.	7.	4.1	3.09	800	500
4	0.	8.2	4.82	3.3	800	500

duration of the ripples on the records of Caleta de Campos. The frequency content of the low-frequency band is limited artificially because of the processing of the accelerograms (Mena *et al.*, 1986). We make the doubly peaked spectra by adding the two initial period bands. We assume that the amplitude of the 3 sec period band is five times smaller than that of the 12 sec period band. This value corresponds to an increase by a factor of 3 of the relative amplitude of the 3 sec period component with respect to the ω^{-2} model, as suggested by Singh *et al.* (1989). The results obtained are presented in Figure 10 for the 3 sec and 12 sec period source excitations and for the complete doubly peaked spectrum. The synthetics are compared with actual vertical displacement records in Mexico City. The computed waveform is now in good agreement with the observations, including the difference in arrival time between the long-period pulse and 3 sec ripples. The actual seismograms show a longer duration due to scattered waves and to waves coming from parts of the fault that broke later. Nevertheless, for the arrivals relevant to the damage (the 3 sec ripples), this computation confirms our consistent interpretation: the ripples correspond to *Lg*. The long-period pulse consists of the fundamental Rayleigh wave. As shown in Figure 10, some stations, as TACY appear to have been triggered by
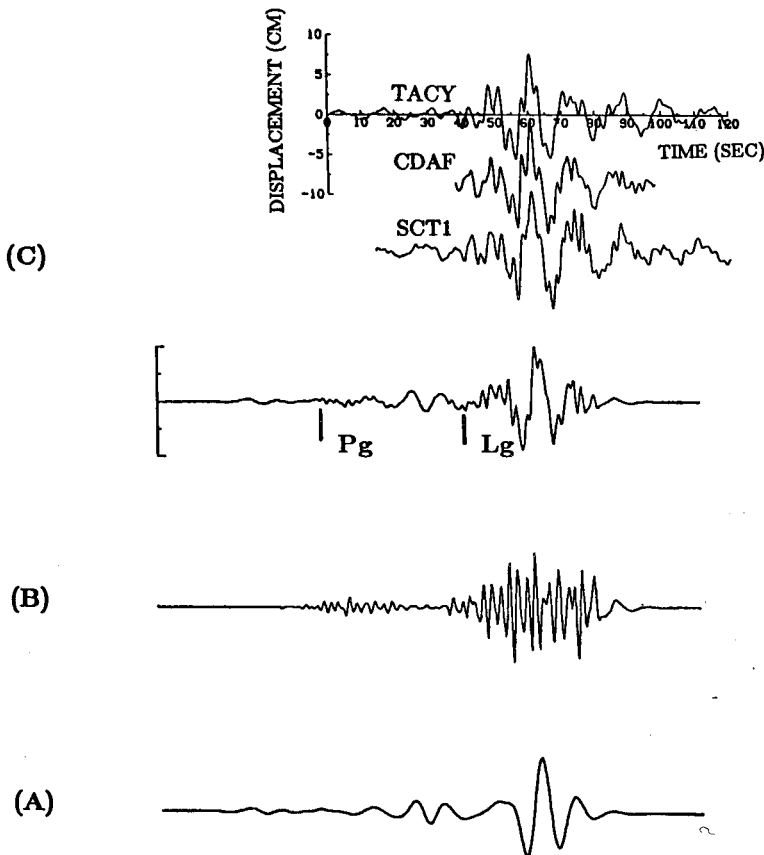

FIG. 10. Synthetic seismograms obtained for the first patch of the rupture using the crustal model without sedimentary layer. (a) and (b) Waveforms obtained for source excitations whose dominant periods are 12 sec and 3 sec, respectively. (c) Waveform obtained with a source excitation that presents a doubly peaked spectra, as described in the text and the comparison with the actual seismograms.

the onset of *Pg* which consists of *P* waves partially trapped in the crust. Other stations, as CDAF, are triggered by the *Lg* wave.

DISCUSSION

Our second interpretation leads to a coherent description of the main features of the rupture process during the Michoacán earthquake and of the wave phenomena between the earthquake source and Mexico City. Following Singh *et al.* (1989), we believe that the destructive 3 sec ripples have been emitted a few seconds after the initiation of the rupture. Seen in the low-frequency domain, the rupture appears to develop as a smooth crack. The ripples can be due to instability of the rupture propagation presenting a pseudo-periodicity. This phenomenon of pseudo-periodic changes of the rupture velocity has been predicted by Ida (1973). Changes of the rupture velocity will result in emission of high-frequency waves that have a very striking directivity (Achenbach and Harris, 1978; Campillo, 1983). During the first stage of the breakage, the rupture front developed essentially in the direction toward the ocean. Therefore, the high frequency waves emitted will present their maximum amplitude toward the ocean. This can explain the relatively low level of peak acceleration observed in the land. The second stage of the rupture consists of the breakage of a second patch at about 82 km southeastward of the epicenter and 26 sec after the initiation (e. g., Houston and Kanamori, 1986). This observation means that the rupture has propagated very rapidly (3.15 km/sec) through the recent failure zone of the 1981 Playa Azul earthquake ($M = 7.3$). This very fast propagation is not associated with strong high-frequency radiation because the stress release was probably very low. Another possibility is that the rupture of the second patch was triggered by the elastic waves radiated from the first. Neither the records in Mexico City nor along the coast allow us to conclude at this point if the second subevent had or had not contributed to the 3 sec period signal observed at Mexico City. Anyway, this contribution does not appear to be prominent. If the rupture at the southern end of the fault is associated with some form of heterogeneous faulting, as suggested by the complexity of the accelerograms recorded in this region, we have no evidence of contribution from this zone to the strong ground motion in Mexico City in the frequency range relevant to the damage.

In the absence of further information on the crustal structure, we favor our second interpretation because it is more consistent with avaliable observations. In any case, it is clear that the exceptional damage in Mexico City requires us to invoke the faulting process which generated enhanced radiation of seismic waves in the period range around 3 sec.

The 3 sec period perturbation emitted during the first stage of the rupture has propagated as guided *S* waves in the crust, namely, *Lg*. These *Lg* waves are the most efficient mode of propagation of seismic energy for the period range (3 sec) and distance range (350 km) relevant to the destruction in Mexico City. This type of propagation results in a significant increase of the duration of the signal: the duration of the ripples in the incident field on the Mexico City basin, as revealed at hillside sites, is longer than the duration observed on the teleseismic or near-source records.

This *Lg* wave train was incident on the Mexico City basin with an amplitude that was not sufficient to represent a real danger for the city; no building collapsed outside of the basin. At this point, we have to take into account the site effects which result in impressive amplification and increase of duration. In the case of *SH* waves, we have shown numerically that the two-dimensional response of a sedimen-

tary basin to *Lg* waves is very similar to its response to vertically incident plane waves (Campillo *et al.*, 1988). Concerning the ground motion in Mexico City, the deep basin, consisting of the so-called pre-Chichinautzin sediments, is responsible for an amplification factor between 3 and 7 in the period range around 3 sec (Bard *et al.*, 1988). These values include two-dimensional effects. The damaged area is located on the lake zone where the soil consists of lacustrine deposits with very low *S*-wave velocity. The fundamental period of resonance of this layer is also close to 3 sec in a large part of the city. When a soft clay layer is added to the model and realistic values of material damping are assigned, the amplification reaches about 20 (Bard *et al.*, 1988). These large scale effects are sufficient to explain the bulk of the seismic response of the basin as shown by Sanchez-Sesma *et al.* (1988), but fail to account for the extreme spatial variability of the damage (Hall and Beck, 1986) and of the records.

In the presence of very soft surficial layer as in Mexico City, the effect of small scale (hundreds of meters) lateral heterogeneity can be important. This type of effect is not usually studied because the details of the structure are not sufficiently known to follow a deterministic approach. Nevertheless, we have shown (Campillo *et al.*, 1989) that small, smooth variations of the surficial structure can produce striking effects. We can expect an increase of amplitude of one order of magnitude in the spectral domain with respect to the case of a flat clay layer even for periods of several seconds. This amplification occurs for the vertical resonance period of the layer, that is a few seconds in Mexico City, and is associated with large increase of the duration. Similarly, local deamplification can also occur. We found that spectral amplitudes can be one order of magnitude different between points only a few hundred meters apart. This may explain the irregular distribution of damage that may be due to lateral variations in the depth of boundary between alluvium and deeper deposits.

Thus, the destructive strong ground motion in Mexico City was the result of a source effect leading to an enhanced radiation at a period of 3 sec, together with a very efficient mode of propagation as *Lg* waves traveled along the path to Mexico City, where the local site conditions result in a multiple resonance of the deep basin, the clay layer, and the buildings. This unfortunate example shows the need to consider simultaneously source, path and site effects in the evaluation of seismic risk. In Mexico, we need to continue to study earthquake source processes in the subduction zone fault system, site effects in Mexico City, and the crustal structure between the earthquake source and Mexico City.

REFERENCES

Achenbach, J. D. and J.G. Harris (1978). Ray method for elastodynamic radiation from a slip zone of arbitrary shape, *J. Geophys. Res.* **83**, 2283–2281.
Aki, K. (1968). Seismic displacement near a fault, *J. Geophys. Res.* **73**, 5358–5376.
Aki, K. (1988). Local site effects on strong ground motion. *Earthquake Engineering and Soil Dynamics II–Recent Advances in Ground Motion Evaluation,"* June 27–30, Park City, Utah.
Aki, K. and P. G. Richards (1980). *Quantitative Seismology*, W. H. Freeman, San Francisco.

Aki, K., S. Stacey, M. Campillo, H. Kawase and F. J. Sanchez-Sesma (1987). Source, path and site effects during the Michoacán earthquake of 1985, AGU Fall Meeting, *EOS* **88**, 1354.

Anderson, J. G., P. Bodin, J. N. Brune, J. Prince, S. K. Singh, R. Quaas, and M. Oñate (1986). Strong ground motion from the Michoacán, Mexico earthquake, *Science* **233**, 1043–1048.

Bard, P. Y., M. Campillo, F. J. Chavez-Garcia, and F. J. Sanchez-Sesma (1988). A theoretical investigation of large-and small-scale amplification effects in the Mexico City valley, *Earthquake Spectra* **4**, 608–633.

Beck, J. L. and J. F. Hall (1986). Factors contributing to the catastrophe in Mexico City during the earthquake of September 18, 1985, *Geophys. Res. Lett.* **13**, 583–586.

Bouchon, M. (1978). Discrete wavenumber representation of elastic wavefields in three dimension space, *J. Geophys. Res.* **84**, 3608–3614.

Bouchon, M. (1981). The rupture mechanism of the Coyote Lake earthquake of August 6, 1978 inferred from near field data, *Bull. Seism. Soc. Am.* **71**, 858–871.

Bouchon, M. and K. Aki (1977). Discrete representation of seismic source wavefields, *Bull. Seism. Soc. Am.* **67**, 258–277.

Campbell, K. W. (1981). Near source attenuation of peak horizontal acceleration, *Bull. Seism. Soc. Am.* **71**, 2038–2070.

Campillo, M. (1983). Numerical evaluation of near-field high-frequency radiation from quasi-dynamic circular faults, *Bull. Seism. Soc. Am.* **73**, 723–734.

Campillo, M., F. J. Sanchez-Sesma, and K. Aki (1989). Influence of small lateral variations of a soft surficial layer, *J. Soil Dyn. Earthquake Eng.* (in press).

Campillo, M., P. Y. Bard, F. Nicollin, and F. J. Sanchez-Sesma (1988). The incident wavefield in Mexico City during the great Michoacán earthquake and its interaction with the deep basin, *Earthquake Spectra* **4**, 581–608.

Das, S. and K. Aki (1977). Fault plane with barriers: a versatile earthquake model, *J. Geophys. Res.* **82**, 5658–5670.

Ekstrom, G. and A. M. Dziewonski (1986). A very broad band analysis of the Michoacán, Mexico earthquake of September 18, 1985, *Geophys. Res. Lett.* **13**, 606–608.

Eissler, H., L. Astiz, and H. Kanamori (1986). Tectonic setting and source parameters of the September 18, 1885 Michoacán, Mexico earthquake, *Geophys. Res. Lett.* **13**, 568–572.

Hall, J. F. and J. L. Beck (1986). Structural damage in Mexico City, *Geophys. Res. Lett.* **13**, 588–582.

Herrmann, R. B. and A. Kijko (1983). Modeling some empirical vertical component *Lg* relations, *Bull. Seism. Soc. Am.* **73**, 157–171.

Houston, H. and H. Kanamori (1986). Source characteristics of the 1985 Michoacán, Mexico, earthquake at period of 1 to 30 seconds, *Geophys. Res. Lett.* **13**, 597–600.

Ida, Y. (1973). The maximum acceleration of strong ground motion, *Bull. Seism. Soc. Am.* **83**, 858–868.

Kasahara, K. (1955). A short discussion on ripples in earthquake shocks: aftershocks of the Boso-Oki earthquake, *Bull. Earthquake Res. Inst., Tokyo Univ.* **33**, 631–640.

Kawashima, K., K. Aizawa, and K. Takahashi (1984). *Proc. VIII World Conference on Earthquake Engineering*, vol. 2, 257–264.

Kostrov, B. Y. (1964). Self similar problems of propagation, *J. Appl. Math. Mech.* **28**, 1077–1078.

Madariaga, R. (1976). Dynamics of an expanding circular fault, *Bull. Seism. Soc. Am.* **66**, 638–666.

Martinez, A. and C. Javier I. (1985). Estudio intensidades and isosistas. Report, UNAM, Mexico City.

Mena, E., C. Carmona, R. Delgado, L. Alcantara, and O. Dominguez (1986). Catalogo de accelerogramas procesados del sismo de Septiembre de 1985, parte I: Ciudad de Mexico, Series del Instituto de Ingeniería No. 487, UNAM, Mexico City.

Mendoza, C. and S. H. Hartzell (1988). Inversion for slip distribution using GDSN P-waves: North Palm Springs, Borah Peak and Michoacán earthquakes, *Bull. Seism. Soc. Am.* **78**, 1082–1111.

Riedesel, M. A., T. H. Jordan, A. F. Sheehan, and P. G. Silver (1986). Moment-tensor spectra of the 18 Sept 85 and 21 Sept 1885 Michoacán, Mexico earthquakes, *Geophys. Res. Lett.* **13**, 608–612.

Romo, M. P. and H. B. Seed (1986). Analytical modeling of dynamic soil response in the Mexico earthquake of September 19, 1985. *Proc. International Conference on the 1985 Mexico earthquakes*, Mexico.

Sánchez-Sesma, F. J., S. Chávez-Pérez, M. Suárez, M. A. Bravo, and L. E. Pérez-Rocha (1988). On the seismic response of the valley of Mexico, *Earthquake Spectra* **4**, 568–588.

Steinhart, J. S. and R. P. Mayer (1961). Explosion studies of continental structure, Publication 822, Carnegie Institution of Washington D.C., 408 pp.

Singh, S. K., A. Mori, E. Mena, F. Kruger, and R. Kind (1989). Evidence for anomalous body-wave radiation between 0.3 to 1 Hz from the September 1985, Michoacán earthquake, *Geophys. J.* (in press).

UNAM Seismology Group (1986). The September 1985 Michoacán earthquakes: aftershocks distribution and history of rupture. *Geophys. Res. Lett.* **13–6**, 573–576.

Valdes, C. M., W. D. Mooney, S. K. Singh, R. P. Meyer, C. Lomnitz, J. H. Luetgert, C. E. Helsley, B. T. R. Lewis, and M. Mena (1986). Crustal structure in Oaxaca, Mexico, from seismic refraction measurements. *Bull. Seism. Soc. Am.* **76**, 547–563.

Yomogida, K. (1988). Crack-like rupture processes observed in near-fault strong motion data. *Geophys. Res. Lett.* **15**, 1223–1226.

Zirbes, M. D., J. M. Lishner, and B. J. Moon (1985). *National Earthquake Information Center Waveform Catalog, September 1985, U.S. Geol. Surv., Open-File Rept. 85–6607*

OBSERVATOIRE DE GRENOBLE
UNIVERSITÉ JOSEPH FOURIER
(UA CNRS 733)
IRIGM
BP53X 38041 GRENOBLE, FRANCE
    (M.C., J.C.G.)

DEPARTMENT OF GEOLOGICAL SCIENCES
UNIVERSITY OF SOUTHERN CALIFORNIA
UNIVERSITY PARK
LOS ANGELES, CALIFORNIA 90089–0740
    (K.A.)

INSTITUTO DE INGENIERÍA
UNAM
COYOACÁN 04510
MÉXICO D.F., MÉXICO
    (F.J.S-S.)